Fibers Segmentation

by Lina Septiana

Submission date: 09-Sep-2022 10:55AM (UTC+0700)
Submission ID: 1895636005
File name: File220823222203220823222203050318098401.pdf (1.64M)
Word count: 4930
Character count: 27135

IIEEJ Paper

Elastic and Collagen Fibers Segmentation Based on U-Net Deep Learning Using Hematoxylin and Eosin Stained Hyperspectral Images

Lina SUSIANA[†], Hiroyuki SUZUKI[††], Masahiro ISHIKAWA[‡](*Member*), Takashi OBI[††], Naoki KOBAYASHI[‡](*Fellow*), Nagaaki OHYAMA[††], Takaya ICHIMURA[‡‡], Atsushi SASAKI[‡‡], Erning WIHARDJO[§], Harry ARJADI[§§]

[†]Tokyo Institute of Technology, Department of Information and Communication Engineering,
[††]Tokyo Institute of Technology, Research Institute for Innovation in Science and Technology,
[‡]Saitama Medical University, Faculty of Health and Medical Care, [‡‡]Saitama Medical University, Faculty of Medicine,
[§]Kristen Duta Wacana Christian University, Faculty of Engineering and Computer Science, Indonesia,
[§§]Indonesian Institute of Sciences, Research Center for Quality System and Testing Technology (P2SMTP-LIPI), Indonesia.

<Summary> In Hematoxylin and Eosin (H&E) stained images, it is difficult to distinguish collagen and elastic fibers because these are similar in color and texture. This study tries to segment the appearance of elastic and collagen fibers based on U-net deep learning using spatial and spectral information of H&E stained hyperspectral images. Groundtruth of the segmentation is obtained using Verhoeff's Van Gieson (EVG) stained images, which are commonly used for recognizing elastic and collagen fiber regions. Our model is evaluated by three cross-validations. The segmentation results show that the combination of spatial and spectral features in H&E stained hyperspectral images performed better segmentation than H&E stained in conventional RGB images compare to the segmentation of EVG stained images as ground truth by visually and quantitatively.

Keywords: pathology image, Hematoxylin Eosin (H&E), Verhoeff's Van Gieson (EVG), U-net, hyperspectral, segmentation

1. Introduction

Specimen staining is one important process in pathology diagnosis. The color information produced from tissue structure can show the tissue condition, which is useful for further analysis. Standard staining methods in pathology diagnosis is Hematoxylin and Eosin (H&E) stain, it is used to show the morphological structure of tissue[1)]. This staining method is always done in histology processing.

An obvious correlation between the abnormality of elastic fibers and diseases was reported in medical papers[2)-4)]. Specifically, it is important for the diagnosis of pancreatic ductal carcinoma to the quantified measurement of specific density and distribution of elastic fibers in the walls of vessels and ducts associated with the tumor phenomenon[4)]. Commonly, Verhoeff's Van Gieson (EVG) stained image is being used to recognize elastic fiber from collagen fiber for pathological diagnosis using microscopic observation. EVG stained images can discriminate elastic and collagen fibers easily with not only human eyes but also computer analysis, because EVG stained images have significant color differences between elastic and collagen fibers. It has been reported that the usage of Linear Discriminant Analysis (LDA) on EVG stained image based on three color features can produce good classification results between elastic and collagen fibers[5)]. However, in pathology diagnosis, the EVG stain is an additional staining method, and it is produced while the H&E stain has been done. It means that to produce the EVG stain needs an extra additional effort than the H&E stain both in the staining process and in cost[6)]. Therefore, we approach the possibility to distinguish elastic fibers from collagen ones using H&E stained images to improve the efficiency in pathology diagnosis.

However, the appearance of elastic fibers is not easy to be recognized from conventional H&E stained RGB image with three color bands due to the similar color and pattern with collagen fibers. Hence we use hyperspectral imaging systems that can analyze tissue samples in more narrow and various wavelength bands than using general RGB cameras. The hyperspectral image provides valuable and comprehensive information about the object characteristic on biomedical tissues[7)-12)], and it can be potentially used to recognize the elastic and collagen fibers from H&E stained images, which might include a small color difference between elastic and collagen regions. Therefore, we investigate the possibility of distinguishing elastic and collagen fibers without EVG stained specimens but with H&E stained ones by applying hyperspectral image analysis.

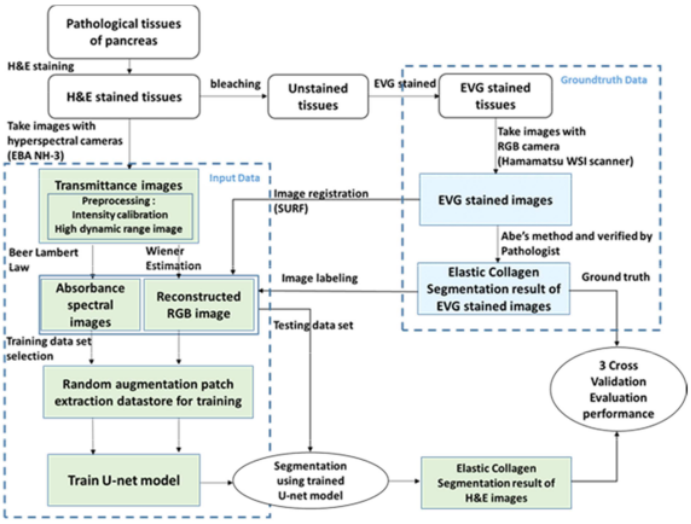

Fig.1 Block diagram of proposed method

In our previous study, we did the pixel-wise ~~tic~~ classification of elastic and collagen fibers from H&E stained hyperspectral images of pancreatic tissues using spectral information, we showed that spectral data was more effective in classifying those elastic and collagen fibers regions by applying Linear Discriminant Analysis (LDA) compare to RGB images.

Continuing our study[12], we consider the fact that commonly elastic fibers exist in specific areas[13], i.e., in blood vessel wall regions. Different from elastic fibers, collagen fibers may exist in almost all connective tissue[13]. Hence the spatial feature provides meaningful information to distinguish elastic and collagen fibers. Beside of that, the previous research by Ushiki[14] had observed the micro-level texture with the high magnification about differences between elastic and collagen fibers. It found some significant differences in basic structure and arrangement between elastic and collagen fibers based on a morphological viewpoint in high-resolution images. It means that the effective differences of textures for elastic and collagen fiber might be shown in normal pathological magnification images (20x)[14)15)]. Besides that, the absorbance intensities of images have different values in every different wavelength, therefore the texture differences of elastic and collagen fibers can be more emphasized in hyperspectral image[16)-18)]. For those reasons, in this study, we propose a pixel-wise classification method using not only spectral features but also the combination of spectral and spatial features of H&E stained hyperspectral images. This method can provide more comprehensive information to increase classification accuracy.

The difficulty of applying the combination of spectral and spatial information to the classification of elastic and collagen fibers is that both features have different scales and units. The use of conventional machine learning method such as Linear Discriminant Analysis (LDA) needs lots of calculations for getting many spatial features in images corresponding to each wavelength to map and to fuse both features. It means hyperspectral images needs much significant processing times compared to RGB images in conventional machine learning method[19),20)].

Refer to the previous study[21)], U-net is a powerful segmentation technique for medical images based on spatial and channel features. The network works by processing spatial and spectral information in contracting and expansive path. U-net enables to train spatial and spectral features automatically without any redundancy from many calculations process as happened in conventional machine learning. U-net also works well using only a few number image samples, with small and thin image boundaries. For these reasons, we employ U-net based architecture to investigate the combination of spectral and spatial features for classification of elastic and collagen fibers using H&E hyperspectral images.

For quantitative evaluation, the segmentation accuracy is confirmed visually and quantitatively by comparing ground truth based on EVG stained images with Abe's method[5)], which have been corrected by the pathologist.

2. Proposed Method

Figure 1 shows the pipeline of our proposed method for elastic and collagen segmentation in the H&E stained

image. Procedures in this study consist of several steps, i.e., image acquisition, preprocessing, training, segmentation, and verification. Details of the above procedures are described in the following sections.

2.1 Image acquisition

Human pancreas tissues of H&E stained specimen and its EVG images were provided by BioMax Inc. These tissues were collected under the highest ethical standards, with the donor being informed completely with their consent and collected under HIPPA approved protocols. Two types of stained images have almost the same biological structures because the EVG stained specimens were obtained by dying unstained specimens that were obtained by bleaching the H&E stained specimens.

H&E hyperspectral images were captured by an optical microscope (Olympus BX-53) with a halogen lamp as the light source and a 61 band hyperspectral camera from EBA Japan NH-3, with 20x magnification, one pixel has dimensions 0.25x0.2758 μm^2, image size is 120x207.4 μm^2 or 480 x 752 pixels, wavelength range is 420nm to 720nm with 5nm wavelength interval. We did intensity calibration to take into account the difference in the spectrum of light sources and generated a high dynamic range image by replacing the overexposure part of the image with the lower one. EVG stained tissues were captured by using Hamamatsu Whole Slide Image (WSI) scanner as RGB image.

To make the object recognition on H&E stained specimen easier to be analyzed, we used absorbance spectral images, which were converted from a captured transmittance hyperspectral images, based on Beer-Lamber law equation as follows[16)-18)],

$$I_{a_i}(\lambda) = -\log\left\{\frac{I_i(\lambda)}{I_{o_i}(\lambda)}\right\}, \quad (1)$$

where $I_{a_i}(\lambda)$ is absorbance spectra, $I_i(\lambda)$ is a captured transmittance spectra, and $I_{o_i}(\lambda)$ incident spectral of i^{th} pixel.

Figure 2 shows the intensity of absorbance spectra from some random pixel points in H&E hyperspectral image, blue and red lines denote elastic and collagen fibers, respectively. Those spectral information show more comprehensive information with small color differences than the RGB images which has only three channel bands.

We also generated H&E stained RGB images from the hyperspectral image by employing Wiener estimation[22)23)], to compare the performance of classification using hyperspectral images to RGB images.

As a pre-process to classify elastic and collagen fiber using H&E stained image, we employ image registration method based on Speed up robust features (SURF)[24)] to trace the fiber region of the EVG image to corresponding

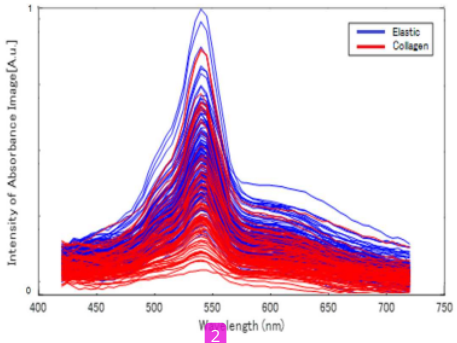

Fig.2 Absorbance spectrum of elastic and collagen samples obtained from H&E stained hyperspectral images

one of an H&E stained image. To obtain the ground truth images, we make segmentation of EVC images using Abe's method[5)] and identified elastic and collagen fiber regions. Two of our author members who are pathologists from Saitama Medical University verified these results, and the appropriateness of Abe's method was confirmed. Thus, we use it to get labels of elastic and collagen fiber.

In this study, we focus on the classification of elastic and collagen fibers only, because it is most difficult for pathologists to distinguish these two components in H&E stained image, which have a very similar color and pattern. The other components, i.e. cytoplasm and nucleus can be recognized easily by pathologists as these have different patterns or colors. For this reason, we extract the region of interests (ROIs), which contain both elastic and collagen fiber areas in H&E stained images by applying Abe's method on EVG stained image which used as a label. After extracting the fiber regions, we classify the elastic and collagen fibers from the ROIs.

2.2 U-net based classification method for spatial-spectral features

In this study, we use a U-net[21),25)] based architecture, as seen in **Fig. 3**. A blue box represents a multi-channel feature map, and a number on the top of each box denotes the number of channels. Another number at the lower-left edge of the box denotes the image size. A white box denotes the copied feature map. The proposed network architecture using 61 feature channels, consists of a downsampling path and an upsampling path. The downsampling path employs 3x3 zero-padded convolutions, which treats the edge area of the input image by zero to keep the patch size as it is. The 3x3 zero-padded convolution is repeated twice for each feature map, and then the convolution results are modulated by a rectified linear unit (ReLU), as shown in the blue arrow

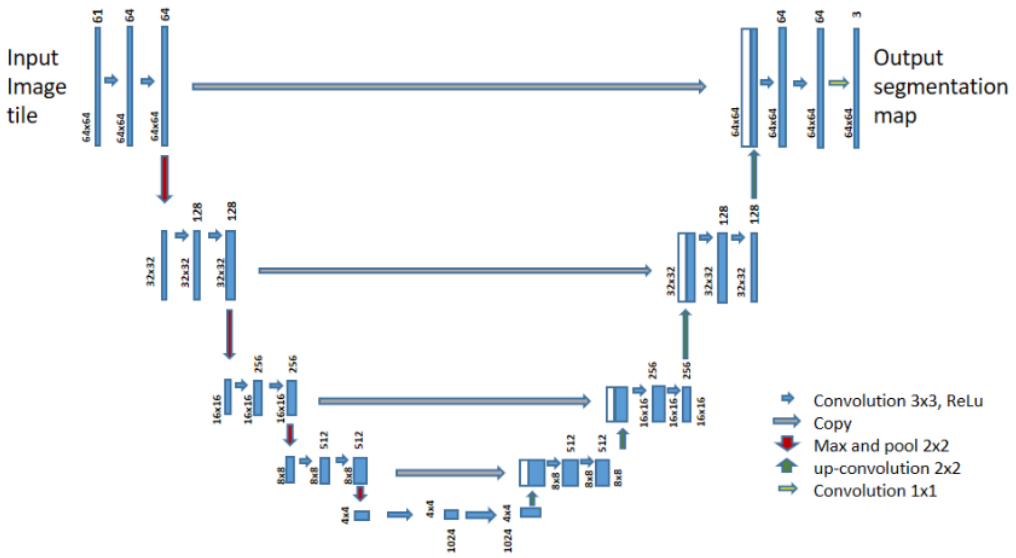

Fig. 3 U-net based architecture for elastin and collagen segmention using H&E stained hyperspectral images

feature

In this process, we extend the number of fearure channels from 61 to 64, because 64 feature channels are standards for U-net architecture[5] , which is commonly used. After that, a 2x2 max pooling operation is employed shown in the red arrow. In the second layer, we double the number of feature channels from 64 to 128 at each downsampling step. For the upsampling path, each step of the feature map is followed by a 2x2 convolution that divides the feature channels number into half, a concatenation with the corresponding feature map from the downsampling path, and two 3x3 convolutions and modulations by a ReLU. At the final layer, a 1x1 convolution is used, it is not looking at anything around itself. It is used only to reduce the number of feature channels.

The details of the U-net based architecture, such as the selected optimum parameters for the histopathology analysis are as follows:

- We use hyperspectral images with 61 channels to feed the U-net architecture. Input images are small patch images, including elastic and collagen fiber regions, which are crapped from H&E stained images. Output images are 3 channels, elastic fiber, collagen fiber, and the other component.
- The filter size for convolution is 3x3. It is the most suitable size to preserve the small and thin structures in the image, according to the previous study[26].
- The patch size is 64 × 64. The smaller size will reduce the accuracy of the machine learning, while the bigger size will increase the processing time as the accuracy is keeping the same level. In this experiment, for each cross-validation, 36 patches are prepared from 2 images (18 patches per image) samples. They are trained randomly as many as 100 and 1,000 patches from those 36 patched data, using reflection and 90-degree rotation augmentation image, it produces 1600, and 16,000 augmentation patches respectively from 100 and 1,000 patches (16 variant patch per image), which effectively increase the segmentation performance with a small number of training data.
- Initial Learning rate 0.001, epoch 5, those for the optimal learning process with the minimum processing time
- We propose to use U-net pre-trained model which was trained using remote sensing multispectral dataset[27] firstly before used in this segmentation[28].

3. Experiments

3.1 Sample tissue mages

We used three sample tissue images for three-fold cross-validations, as shown in **Fig. 4**. In the figure, group(a) and group(b) show H&E stained images and EVG

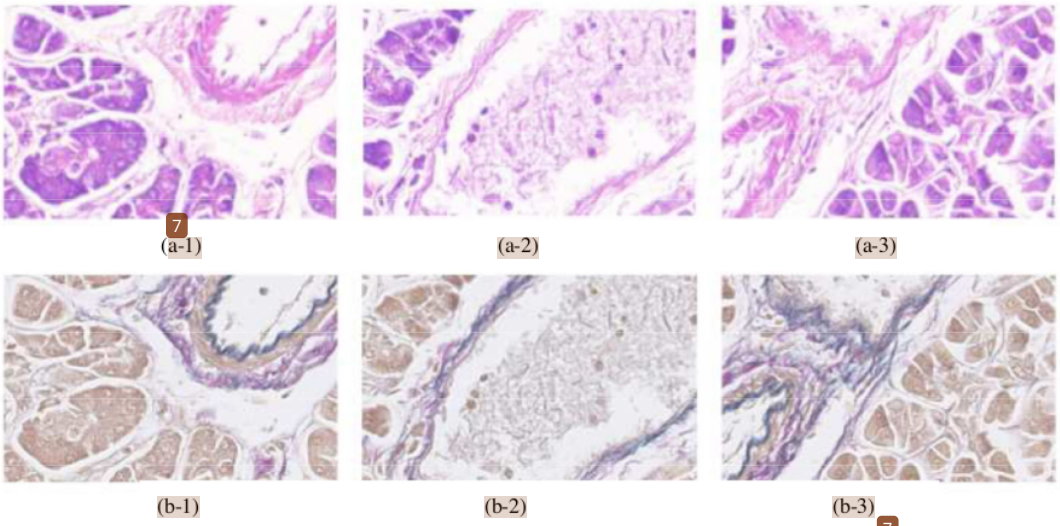

Fig. 4 H&E stained images of sample 1,2,3: (a-1), (a-2), (a-3); and EVG stained images of sample 1,2,3:(b-1), (b-2), (b-3)

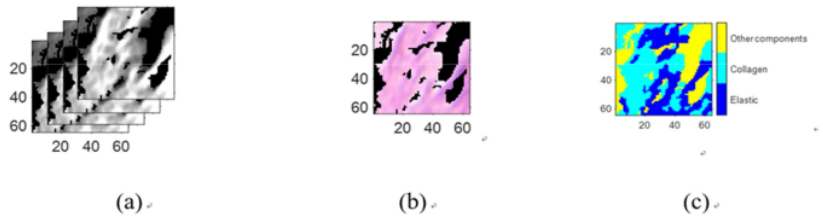

Fig. 5 64 × 64 patch (a) Hyperspectral image (4 band images are extracted from 61 band ones), (b) corresponding RGB image, (c) Label

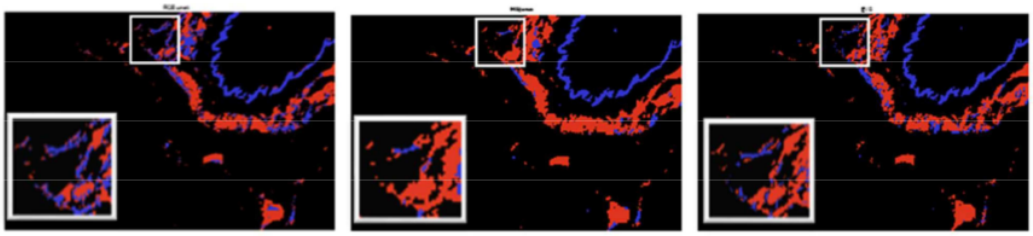

Fig. 6 Cross-validation 1 segmentation result (a) RGB image, (b) Hyperspectral image, (c) Groundtruth image

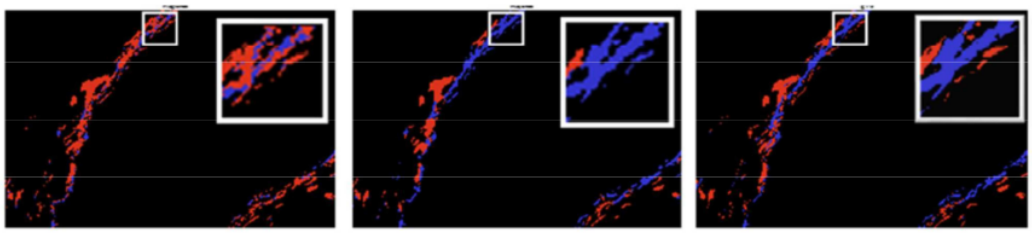

(a) (b) (c)

Fig. 7 Cross-validation 2 segmentation result: (a) RGB image, (b) Hyperspectral image, (c) Groundtruth image

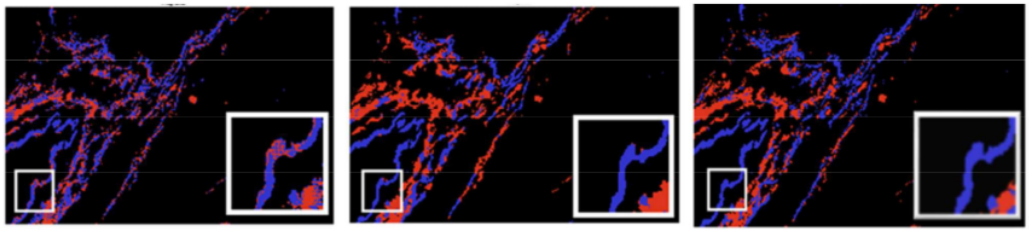

(a) (b) (c)

Fig. 8 Cross-validation 3 segmentation result: (a) RGB image, (b) Hyperspectral image, (c) Groundtruth image

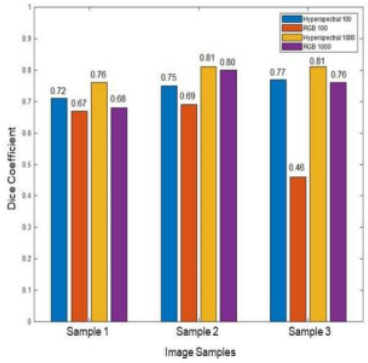

Fig. 9 Dice coefficients of hyperspectral and RGB images using spectral-spatial features (U-net)

stained images, respectively. We used three images for cross-validations as follows,

- Cross-validation 1: we extract the fiber area from samples 2 and 3, then be tested in sample 1.
- Cross-validation 2: we extract the fiber area from samples 1 and 3, then be tested in sample 2.
- Cross-validation 3: we extract the fiber area from samples 1 and 2, then be tested in sample 3.

Training process use parameter mentioned in section 2.2. **Figure 5** (a)-(c) show examples of 64×64 patch of a hyperspectral image, a corresponding RGB image, and its label, respectively. The label in (c) consists of three classes, i.e., elastic, collagen, and other components obtained by applying Abe's method to EVG stained images[5] and corrected by the pathologist.

3.2 Segmentation result

We obtained segmentation results of elastic and collagen fiber regions using three cross-validations. We compared the segmentation result of the hyperspectral images to the conventional RGB images.

Figure 6, 7 and **8** show the results of segmentation using cross-validation 1,2 and 3, respectively. In each figure, (a) and (b) denote segmentation result images obtained from hyperspectral and RGB images, respectively, and (c)

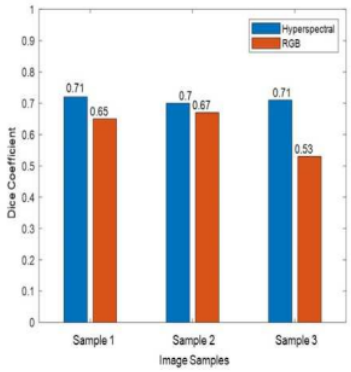

Fig. 10 Dice coefficients of hyperspectral and RGB images using spectral features (LDA)

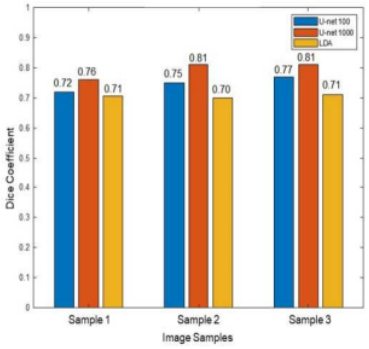

Fig. 11 Dice coefficients of hyperspectral images using spectral-spatial features (U-net) and spectral features (LDA)

denotes a ground truth image obtained from EVG stained image[5]. The blue and red color represents elastic and collagen fiber, respectively. These results show that RGB results have more misclassification than hyperspectral images compared to ground truth images.

We also evaluate the segmentation results quantitatively by calculating the classification accuracy using the following equation[29],

$$\text{Dice Coefficient} = \frac{2TP}{2TP+FP+FN} \qquad (2)$$

True Positive (TP) is the number of pixels where elastic fibers are decided as elastic fiber correctly, False Positive (FP) is the number of pixels where collagen fibers are decided as elastic fibers incorrectly, and False Negative (FN) is the number of pixels where elastic fibers are decided as collagen fibers incorrectly in the segmented images.

red bars show the dice coefficients of RGB images for 100 patches, yellow bars show the dice coefficients of hyperspectral images for 1,000 patches, and purple bars show the dice coefficients of RGB images for 1,000 patches. From these data, we can see that the proposed U-net using hyperspectral images performs better than RGB both using 100 and 1,000 patch numbers.

4. Discussion

In section 3, it has been observed that the proposed method has a significantly better performance than RGB images . Also, we compared the proposed method based on spectral-spatial features to the previous sudy based on spectral features [12].

Table 1 Average learning time

Number of patch images	Average learning time
100	200 [sec]
1,000	1,850 [sec]

Figure 10 shows the dice coefficients of hyperspectral and RGB images using spectral features with LDA. Blue bars show the dice coefficient of the hyperspectral images, and red bars show the dice coefficient of RGB images.

Figure 11 shows the dice coefficients of hyperspectral images using spectral-spatial features with U-net and hyperspectral images using spectral features with LDA. Blue and red bars show the dice coefficients of U-net using 100 and 1000 patches, respectively, and yellow bars show the dice coefficients of LDA.

These results indicate that the segmentation of elastic and collagen fibers using hyperspectral images perform better results than RGB images in case of both using the spectral feature only and the combination of spectral-spatial features. In a comparison of spectral-spatial features with U-net and spectral features with LDA, the former ones can classify the elastic and collagen fiber regions with better accuracy. These results were also subjectively evaluated by pathologists from Saitama Medical University, and they gave comments that the segmented images were almost equivalent to the diagnostic outcome by pathologists, and the results of spectral-spatial features with U-net were especially well-classified.

Table 1 shows the average learning time for validations in this experiment. The software for calculation is Matlab 2019a, and the processor is NVIDIA™ Titan X. This result shows that 1000 patch images take more than 9 times of 100 patch images, whereas data size of training is 10 times.

This experiment is our first trial for the segmentation of elastic and collagen fibers. Thus, the developed U-net might have much room to improve because we have tried only a few kinds of parameters such as the architecture of U-net, type of input data, number of training data set, and so on. If we will repeat more trial-and-errors, it is sure that the accuracy will increase.

5. Conclusion

In H&E stained images, it is difficult to distinguish collagen and elastic fibers because these are similar in color and texture.This study observed the segmentation of elastic and collagen fibers from the H&E stained images through hyperspectral transmittance using U-net based spectral-spatial analysis. Groundtruth of the segmentation is obtained using EVG stained images, which are commonly used for recognizing elastic and collagen fiber regions. Our model is evaluated by three cross-validations. The segmentation results show that the combination of spatial and spectral features in H&E stained hyperspectral images performed better segmentation than H&E stained conventional RGB images both in visual appearance and quantitative verification.

This method is not only for visualization but also for pixel wise classification. We believe that this method may help the diagnostic accuracy increase.

Acknowledgment

The authors appreciate to Indonesia Endowment Fund for Education (LPDP) and Join research program between Japan Society for the Promotion of Science (JSPS) and Indonesian Institute of Sciences (LIPI), for providing financial support.

References

1) M. Titford: "The Long History of Hematoxylin", Biotechnic & Histochemistry. Vol.80 , No.2, pp.73–78 (2005).
2) J. Uitto, L. Ryhanen, P.A. Abraham, A.J. Perejda: "Elastin in Diseases", The Journal of Investigative Dermatology, Vol. 79, Issue 1, Supplement, pp.160–168 (1982).
3) Y. Yasui, T. Abe, M. Kurosaki, M. Higuchi, Y. Komiyama, T. Yoshida, T. Hayashi, K. Kuwabara, K. Takaura, N. Nakakuki, H. Takada, N. Tamaki, S. Suzuki, H. Nakanishi, K. Tsuchiya, J. Itakura, Y. Takahashi, A. Hashiguchi, M. Sakamoto, N. Izumi: "Elastin Fiber Accumulation in Liver Correlates with the Development of Hepatocellular Carcinoma", PloS one, Vol.11, No.4, e0154558 (2016).
4) E.Lakiotaki, S. Sakellariou, K, Evangelou, G. Liapis, E. Patsouris, I. Delladetsima, Vascular and Ductal Elastotic Change in Pancreatic Cancer, Acta Pathologica, Microbiologica et Immunologica Scandinavica, John Wiley and Son (2015).
5) T. Abe, A. Hashiguchi, K. Yamazaki, H. Ebinuma, H. Saito, H. Kumada, N. Izumi, N. Masaki, M. Sakamoto: "Quantification of Collagen and Elastic Fibers Using Wholeslide Images of Liver Biopsy Specimens", Pathology International Vol.63, Issue 6, pp 305–310, QA, June (2013).
6) www.polyscience.com, accessed on 12 October (2019)
7) M. Ishikawa, C. Okamoto, K. Shinoda, H. Komagata, C. Iwamoto, K. Ohuchida, M. Hashizume, A. Shimizu, N. Kobayashi: "Detection of Pancreatic Tumor Cell Nclei via a Hyperspectral Analysis of Pathological Slides Based on Stain Spectra",Biomedical Optics Express, Vol. 10, No. 9, pp.4568–4588 (2019).
8) D. L. Farkas, C. Du, G. W. Fisher, C. Lau, W. Niu, E. S. Wachman, R. M. Levenson: "Non-invasive Image Acquisition and Advance Processing in Optical Bioimaging", Computerized Medical Imaging and Graphics Vol. 22, No.2, pp.89–102 (1998).
9) B. C. Wilson, S. L. Jacques: "Optical Reflectance and Transmittance of Tissues: Principles and Applications", IEEE Journal of Quantum Electronics; Vol.26, Issue 12, pp.2186–98 (1990).
10) G. Lu, J. V. Little, X. Wang, H. Zhang, M. R. Patel, C. C. Griffith, M. W. El-Deiry, A. Y. Chen, B. Fei: "Detection of Head and Neck Cancer in Surgical Specimens using Quantitative Hyperspectral Imaging", Clin Cancer Res.; 23(18): pp.5426–5436. September 15 (2017).
11) P. A. Bautista, T. Abe, M. Yamaguchi, Y. Yagi, N. Ohyama: "Digital Staining for Multispectral Images of Pathological Tissue Specimens Based on Combined Classification of Spectral Transmittance", Computerized Medical Imaging and Graphics Vol.29, Issue 8, pp. 649–657 (2005).
12) L. Septiana, H. Suzuki, M. Ishikawa, T. Obi, N. Kobayashi, N. Ohyama, T. Ichimura, A. Sasaki, E. Wihardjo, D. Andiani: "Elastic and Collagen Fibers Discriminant Analysis using H&E Stained Hyperspectral Images", Journal of Optical Review, Vol. 26, Issue 4, pp. 369–379. Springer (2019).
13) V. P. Eroschenko, S. H. Mariano: "DiFiore's Atlas of Histology with Functional Correlations", 12th ed. Philadelphia, PA: Wolter Kluwer Health/Lippincott Williams and Wilkins (2013).
14) T. Ushiki, Collagen Fibers: "Reticular Fibers and Elastic Fibers. A Comprehensive Understanding from a Morphological Viewpoint", Arch. Histol. Cytol., Vol. 65, No. 2 (2002).
15) T. L. Sellaro, R. Filkins, C. Hoffman, J. L. Fine, J. Ho, A. V. Parwani, L. Pantanowitz, M. Montalto: "Relationship between Magnification and Resolution in Digital Pathology Systems", Journal of Pathology Informatics, (22 Aug.) Wolters Kluwer-Medknw (2013).

16) D. L. Omucheni, K. A. Kaduki, W. D. Bulimo, H. K. Angeyo: "Application of Principal Component Analysis to Multispectral-Multimodal Optical Image Analysis for Malaria Diagnostics", Malaria Journal, 13:485 (2014).
17) L. Septiana, H. Suzuki, M. Ishikawa, T. Obi, N. Kobayashi, N. Ohyama: "Staining Adjustment of Dye Amount to Clarify the Appearance f Fiber, Nuclei, and Cytoplasm in HE-stained Pathological Kidney Tissue Image", International Multidiciplinary Conference and Productivity and Sustainability, Ukrida press (2017).
18) T. Abe, Y. Murakami, M. Yamaguchi, N. Ohyama, Y. Yagi : "Color Correction of Pathological Images Based on Dye Amount Quantification", Optical Review 12: 293 (2005).
19) H. Yuan, Y. Y. Tang, Y. Lu, L. Yang, H. Luo: "Spectral-Spatial Classification of Hyperspectral Image Based on Discriminant Analysis", IEEE Journal of Selected Topics in Applied Earth Obsevations and Remote Senssing Vol. 7, Issue 6, pp.2035–2043, June (2014).
20) M. Fauvel, J. A. Benediktsson, J. Chanussot, J. R. Sveinsson: "Spectral and Spatial Classification of Hyperspectral Data Using SVMs and Morphological Profiles", IEEE Trans. on Geoscience and Remote Sensing, Vol.46, No.11, November (2008).
21) O. Ronneberger, P. Fischer, T. Brox: "U-Net: Convolutional Networks for Biomedical Image Segmentation", Computing Research Repository (CoRR), abs/1505.04597 (2015).
22) M. Stokes, M. Anderson, S. Chandrasekar, R. Motta: "A Standard Default Color Space for the Internet sRGB", Microsoft and Hewlett-Packard Joint Report, November 5 (1996).
23) H. L. Shen, P. Q. Cai, S. J. Shao, J. H. Xin : "Reflectance reconstruction for multispectral imaging by adaptive Wiener estimation", Optics Express, Vol 15, Issue.23, pp.15545-15554, Nov. (2007).
24) Mathwork. (2018). "Computer Vision System Toolbox Documentation" (r2018). Retrieved December 15, (2018).
25) Mathwork, (2019). "Semantic Segmentation of Multispectral Images using Deep Learning", Image Processing Toolbox document R2019a.Retrieved March 28, (2019).
26) P. S. Chavez, B. Bauer: "An Automatic Optimum Kernel-Size Selection Technique for Edge Enhancement", Remote Sensing Of Environment Vol.12, Issue 1, pp.23–38 (1982).
27) http://www.cis.rit.edu/~rmk6217/rit18_data.mat, Retrieved December 28, (2018).
28) R. Kemker, C. Salvaggio, C. Kanan: "High-Resolution Multispectral Dataset for Semantic Segmentation", Computing Research Repository (CoRR), abs/1703.01918. (2017).
29) A. A. Taha, A. Hanbury: "Metrics for Evaluating 3D Medical Image Segmentation: Analysis, Selection, and Tool", BMC Medical Imaging 15:29, (2015).

(Received July 27, 2019)
(Revised December 24, 2019)

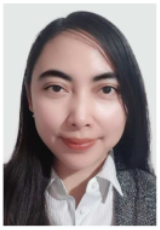

Lina SEPTIANA
She received B.Eng degree from Electronic Eng. Dept., Satya Wacana Christian Univ., Indonesia. M. Sc degree from Electrical Eng. and Computer Science Dept., Chung Yuan Christian Univ., Taiwan. Currently, she is a doctoral student in Information and Communication Eng. Dept. Tokyo Institute of Technology, Japan, and Lecturer at Engineering and Computer Science Fac. Krida Wacana Christian Univ. Indonesia.

Hiroyuki SUZUKI
He received B.E., M.E., and Ph.D. degree from Tokyo Inst. of Tech. in 1998, 2000, and 2006, respectively. He was a Reseacher from 2003 to 2016. He has been an Assistant Professor with Institute of Innovative Research, Tokyo Inst. of Tech since 2016. His research interests include optical information security, hologram, biometric authentication, and medical healthcare information system.

Masahiro ISHIKAWA *(Member)*
He received a Ph.D degree from Niigata University, Japan in 2006. He is currently an Assistant Professor at the Saitama Medical University. His current research interests include image processing and computer aided diagnosis.

Takashi OBI
He earned B.S. degree in Physics, M.S. and Ph.D. degree in Information Physics from Tokyo Inst. of Tech, Japan in 1990, 1992, and 1996 respectively. Currently, he is an Associate Professor of Laboratory for Future Institute of Innovative Research, Tokyo Inst. of Tech. His Research focuses on medical informatics, information system and security, etc. He is a member of IEICE, JAMIT, JSAP, JSNM, JSMP, and IEEE.

Naoki KOBAYASHI *(Fellow)*
He earned B.Sc., M.E. degree from Tokyo Inst. of Tech, in 1979, 1981 respectively. Ph. D degree from Niigata Univ in 2000. He worked for NTT Lab. In 1981-2008. He has been at professor at School of Biomed. Eng, Fac. of Health and Medical Care, Saitama Medical Univ. since 2008. His research interests include medical image processing, image compression, and biosignal processing, He is a member of IECE, IIEEJ, JSMBE, and IEEE.

Nagaaki OHYAMA

He earned Doc. Eng. degree in Information Physics from Tokyo Inst. of Tech. in 1982. His academic career on Tokyo Inst. of Tech has been started since 1982. Become professor in Tokyo Inst. of Tech since 1993. His current research project is related to Japan government's information policy (formulation of electronic preservation standards for medical images, onlin request for claims, introduction of public personal authentication service, etc.)

Takaya ICHIMURA

He earned M.D., Ph.D. degress and is an assistant professor of the Saitama Medical University. He received the Ph.D. degree from Kumamoto University, Kumamoto, Japan, in 2005. His current research interests include nuclear atypia and the molecular nature of chromatin.

Atsushi SASAKI

He earned M.D., Ph.D. degrees from Gunma Univ. School of Medicine in 1980, 1984, respectively. He received the Neuropathology Best Paper Award in 2001, Brain Tumor Pathology Best Paper Award in 2002. He is currently a professor at the Dept. of Pathology, Saitama Medical Univ. His research interests include brain tumor pathology and microglia. Dr. Sasaki is a member of the International Society of Neuropathology and American Association of Neuropathologists.

Erning WIHARDJO

He earned B.Sc., M.Sc. in Physics from Padjajaran Univ. Indonesia in 1976. M. Eng in Opto-Electronics, Univ. of Indonesia in 1979. M. Eng., Doc. Eng. in Physical Information from Tokyo Inst. of Tech. in 1983 and 1986 respectively. He was a scientist at the Indonesia Inst. of Science and Polycore Optical. Ltd., Singapore in 1986-1995. He continued his career at Hoya Lens Ltd in 1995-2012, with the latest position as Director of Hoya Asia H.Q, Singapore. He was awarded professorship from the He Univ. of Ophthalmology and Visual Science, China in 2008. He is the president of Krida Wacana Christian. Univ. Indonesia 2016 - 2020.

Harry ARJADI

He is a senior scientist at Indonesian Institute of Sciences, Research Center for Quality System and Testing Technology (P2SMTP-LIPI), Indonesia. He earned B.Sc., in Physical Eng. from Bandung Inst. of Tech. Indonesia in 1981, M. Sc. In Electronic Intrumentation Design, Ph. D. in Bio-Electromagnetic from Salford Univ. U.K. in 1988 and 1992 respectively.

Fibers Segmentation

ORIGINALITY REPORT

19%	14%	10%	0%
SIMILARITY INDEX	INTERNET SOURCES	PUBLICATIONS	STUDENT PAPERS

PRIMARY SOURCES

1	www.jstage.jst.go.jp Internet Source	7%
2	api.openalex.org Internet Source	2%
3	S.S. Suganthi, S. Ramakrishnan. "Anisotropic diffusion filter based edge enhancement for segmentation of breast thermogram using level sets", Biomedical Signal Processing and Control, 2014 Publication	1%
4	Eleni ALOUPOGIANNI, Hiroyuki SUZUKI, Takaya ICHIMURA, Atsushi SASAKI et al. "**Binary Malignancy Classification of Skin Tissue Using Reflectance and Texture Features from Macropathology Multi-Spectral Images**", IIEEJ Transactions on Image Electronics and Visual Computing, 2019 Publication	1%
5	"Statistical Atlases and Computational Models of the Heart. Atrial Segmentation and LV	1%

Quantification Challenges", Springer Science and Business Media LLC, 2019
Publication

6	"Computational Pathology and Ophthalmic Medical Image Analysis", Springer Science and Business Media LLC, 2018 Publication	1 %
7	air.repo.nii.ac.jp Internet Source	1 %
8	www.ncbi.nlm.nih.gov Internet Source	1 %
9	Shih-Yu Chen, Yu-Chih Cheng, Wen-Long Yang, Mei-Yun Wang. "Surface Defect Detection of Wet-Blue Leather using Hyperspectral Imaging", IEEE Access, 2021 Publication	1 %
10	arxiv.org Internet Source	<1 %
11	"Information Processing in Medical Imaging", Springer Nature, 2017 Publication	<1 %
12	Lakiotaki, Eleftheria, Stratigoula Sakellariou, Kostantinos Evangelou, George Liapis, Efstratios Patsouris, and Ioanna Delladetsima. "Vascular and ductal elastotic changes in pancreatic cancer", Apmis, 2015. Publication	<1 %

13	easychair.org Internet Source	<1%
14	www.coursehero.com Internet Source	<1%
15	www.researchgate.net Internet Source	<1%
16	"Medical Image Computing and Computer Assisted Intervention – MICCAI 2018", Springer Nature America, Inc, 2018 Publication	<1%
17	docksci.com Internet Source	<1%
18	ssl.linklings.net Internet Source	<1%
19	"Artificial Intelligence in Radiation Therapy", Springer Science and Business Media LLC, 2019 Publication	<1%
20	Zhen Liu, Qiang Liu, Gui-ai Gao, Chan Li. "Optimized spectral reconstruction based on adaptive training set selection", Optics Express, 2017 Publication	<1%
21	embs.papercept.net Internet Source	<1%

22	oa.upm.es Internet Source	<1%
23	researchr.org Internet Source	<1%
24	www.saujs.sakarya.edu.tr Internet Source	<1%
25	P. A. Bautista, Y. Yagi. "Digital staining for histopathology multispectral images by the combined application of spectral enhancement and spectral transformation", 2011 Annual International Conference of the IEEE Engineering in Medicine and Biology Society, 2011 Publication	<1%
26	Pinky A. Bautista, Yukako Yagi. "Multispectral Enhancement towards Digital Staining", Analytical Cellular Pathology, 2012 Publication	<1%

Exclude quotes	On	Exclude matches	Off
Exclude bibliography	On		